Figure S1

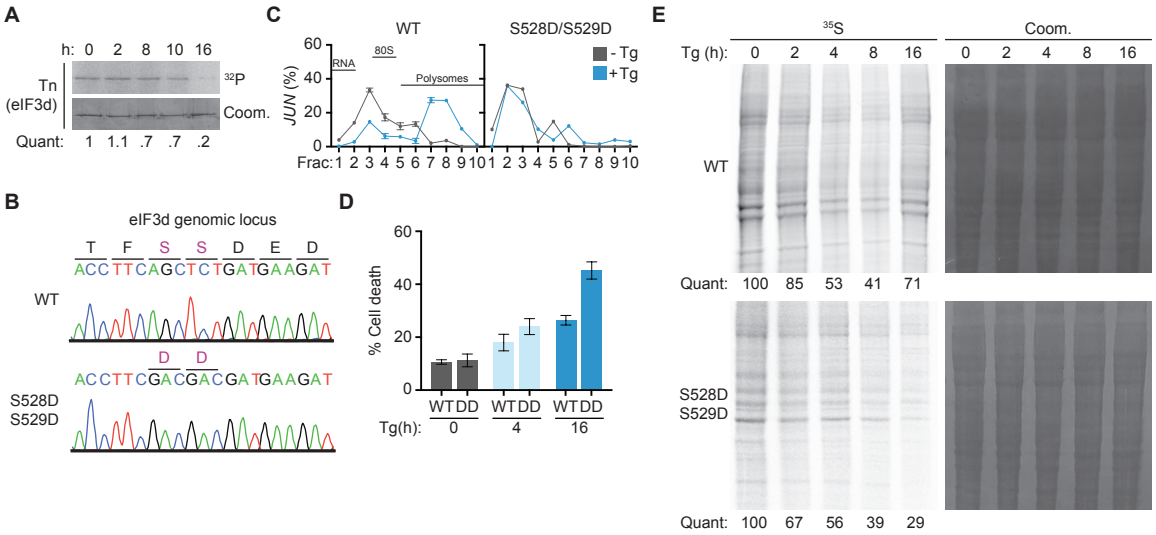
A
h: 0 2 8 10 16
Tn (eIF3d)
32P
Coom.
Quant: 1 1.1 .7 .7 .2
C
WT
S528D/S529D
- Tg
+Tg
RNA
80S
Polysomes
JUN (%)
Frac:1 2 3 4 5 6 7 8 9 10 1 2 3 4 5 6 7 8 9 10
B
eIF3d genomic locus
T F S S D E D
ACCTTCAGCTCTGATGAAGAT
WT
D D
ACCTTCGACGACGATGAAGAT
S528D
S529D
D
% Cell death
WT DD WT DD WT DD
Tg(h): 0 4 16
E
35S
Coom.
Tg (h): 0 2 4 8 16 0 2 4 8 16
WT
Quant: 100 85 53 41 71
S528D
S529D
Quant: 100 67 56 39 29

Figure S1. Cell viability and protein synthesis is dysregulated in cells expressing phosphomimetic eIF3d during chronic ER stress, related to Figure 1. (**A**) Phosphorylation of eIF3 subunits after treatment with tunicamycin (Tn). The phosphor image is representative of three independent experiments. (**B**) Sanger sequencing validation of genome editing to introduce coding changes S528D/S529D in the eIF3d genomic region of HEK293T cells. Shown is chr22 (-): 36,511,540–36,511,560. (**C**) Association of *Jun* mRNA with translation complexes in eIF3d cell lines. *Jun* abundance is expressed as a percentage of the transcripts summed from all fractions and plotted as the mean ± s.d. from a representative quantitative reverse transcription polymerase chain reaction (qRT-PCR) performed in technical duplicate. Blue, Tg-treated cells; gray, untreated cells. WT, wild-type; DD, S528D/S529D. The results are representative of two biological replicates. (**D**) Percentage cell death of eIF3d cell lines upon treatment with Tg at annotated time points. Results are represented as the mean ± s.d. of three independent experiments. (**E**) [^{35}S]-methionine/cysteine labeling shows that HEK293T expressing phosphomimetic eIF3d are unable to restore partial global translational recovery at 16 h treatment with Tg. Phosphorimage of SDS–PAGE gel (^{35}S) is shown resolving total cellular protein synthesis. Coomassie staining of the gel is shown as a loading control. Quantification (Quant.) of gel lane intensity is represented as fold change to cells at 0 h. The results are representative of two independent experiments.

Figure S2

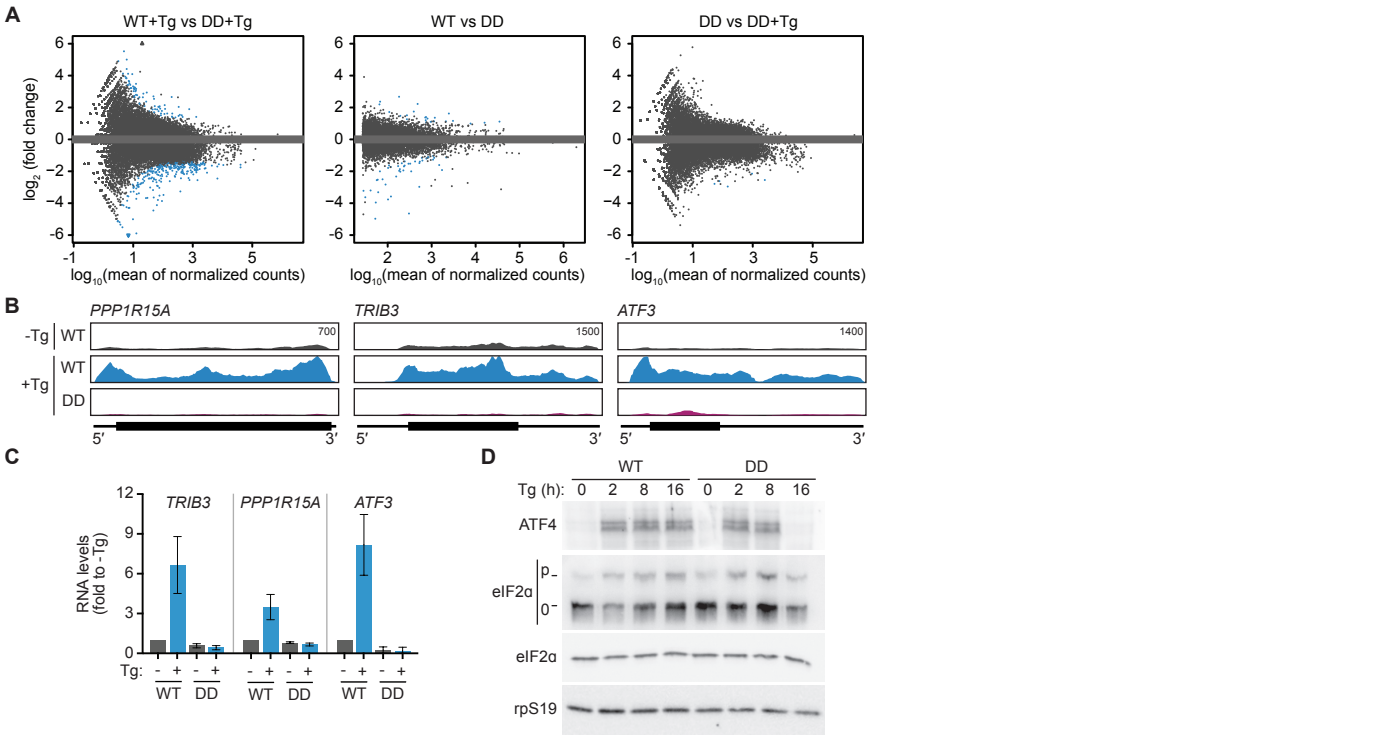
A
WT+Tg vs DD+Tg
WT vs DD
DD vs DD+Tg
log2 (fold change)
log10(mean of normalized counts)
B
PPP1R15A
TRIB3
ATF3
-Tg
+Tg
WT
DD
700
1500
1400
5′
3′
C
TRIB3
PPP1R15A
ATF3
RNA levels (fold to -Tg)
Tg:
WT
DD
D
WT
DD
Tg (h): 0 2 8 16 0 2 8 16
ATF4
eIF2α
p-
0-
eIF2α
rpS19

Figure S2. Validation of dysregulated integrated stress response in cells expressing phosphomimetic eIF3d, related to Figure 1. (**A**) MA plot comparing transcript expression level changes in cells expressing phosphomimetic (DD) or WT eIF3d with or without ISR induction. Genes with significant changes to expression (*P*adj ≤ 0.1) are colored blue. (**B**) Read mapping of transcripts downregulated in HEK293T cells expressing phosphomimetic eIF3d (DD) versus wild-type (WT) cells upon integrated stress response (ISR) induction with thapsigargin (Tg). (**C**) Fold change in transcript expression levels in HEK293T expressing eIF3d mutants upon ISR induction. Results are normalized to untreated WT cells and represented as the mean ± s.d. of three independent experiments. Tg treatments in (A–C) were performed for 16 h. (**D**) Immunoblot of ISR signaling cascade reveals temporal requirements for activated eIF3d. The results are representative of three independent experiments.

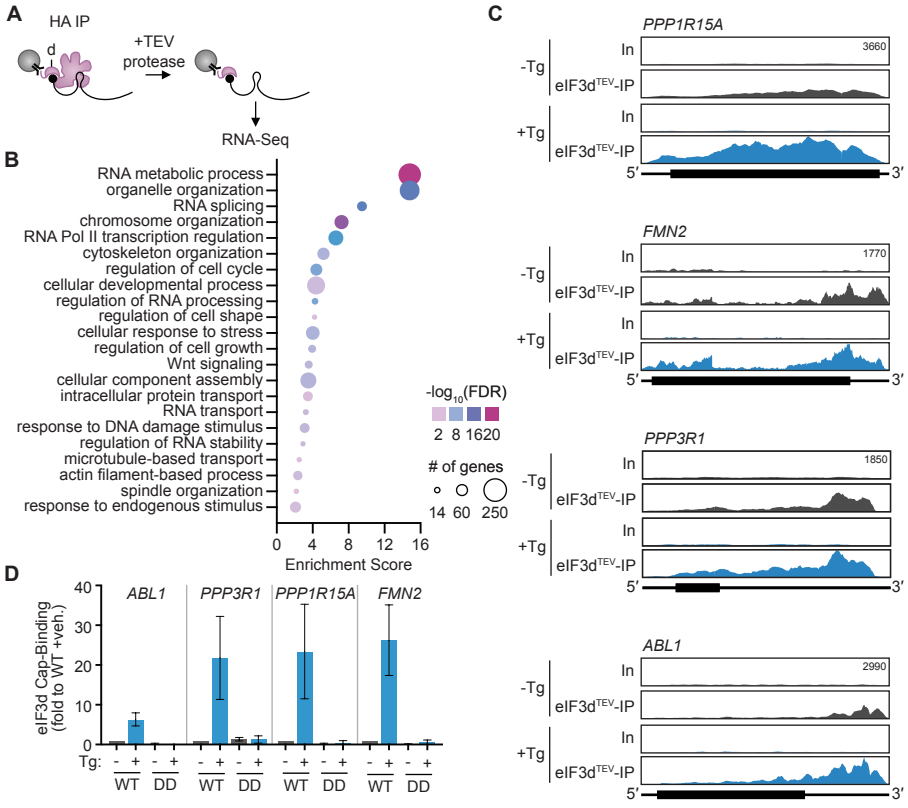
A
HA IP
+TEV protease
RNA-Seq
B
RNA metabolic process
organelle organization
RNA splicing
chromosome organization
RNA Pol II transcription regulation
cytoskeleton organization
regulation of cell cycle
cellular developmental process
regulation of RNA processing
regulation of cell shape
cellular response to stress
regulation of cell growth
Wnt signaling
cellular component assembly
intracellular protein transport
RNA transport
response to DNA damage stimulus
regulation of RNA stability
microtubule-based transport
actin filament-based process
spindle organization
response to endogenous stimulus
0 4 8 12 16
Enrichment Score
-log10(FDR)
2 8 16 20
# of genes
14 60 250
C
PPP1R15A
FMN2
PPP3R1
ABL1
-Tg
+Tg
In
eIF3d^TEV-IP
5′
3′
3660
1770
1850
2990
D
eIF3d Cap-Binding (fold to WT +veh.)
ABL1
PPP3R1
PPP1R15A
FMN2
Tg:
WT
DD

Figure S3. eIF3d^{TEV} Subunit-Seq identifies cap-binding targets involved in the ISR, related to Figure 2. (**A**) Schematic of eIF3d^{TEV} Subunit-Seq approach. (**B**) Gene ontology analysis of eIF3d targets from Tg-treated cells. (**C**) Read mapping to respective target transcripts identified by eIF3d^{TEV} Subunit-Seq during ISR induction. (**D**) eIF3d binding to the 5′ cap of target mRNAs. WT, wild-type; DD, S528D/S529D eIF3d. Cap-binding is normalized to untreated WT cells and represented as the mean ± s.d. of three independent experiments.

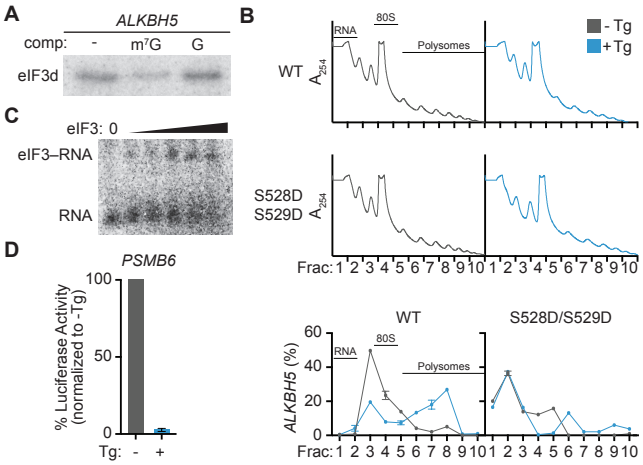
A
ALKBH5
comp: - m7G G
eIF3d
B
RNA
80S
Polysomes
- Tg
+ Tg
WT
A254
S528D
S529D
Frac: 1 2 3 4 5 6 7 8 9 10 1 2 3 4 5 6 7 8 9 10
C
eIF3: 0
eIF3–RNA
RNA
D
PSMB6
% Luciferase Activity (normalized to -Tg)
100
50
0
Tg: - +
WT
S528D/S529D
ALKBH5 (%)
60
40
20
0
Frac: 1 2 3 4 5 6 7 8 9 10 1 2 3 4 5 6 7 8 9 10

Figure S4. eIF3d-mediated translational control of *ALKBH5* requires 5′ UTR RNA structure, related to Figure 3. (**A**) Specificity of *in vitro* eIF3d crosslinking to the 5′ cap structure of the *ALKBH5* 5′ UTR. m^7G, m^7GpppG; G, GpppG. The results are representative of three independent experiments. (**B**) Association of *ALKBH5* mRNA with translation complexes in eIF3d cell lines. *ALKBH5* abundance is expressed as a percentage of the transcripts summed from all fractions and plotted as the mean ± s.d. Blue, Tg-treated cells; gray, untreated cells. WT, wild-type; DD, S528D/S529D. The results are representative of two biological replicates. (**C**) Representative native gel shift showing binding of recombinant eIF3 and *ALKBH5* 5′ UTR RNA. Result is representative of three independent experiments. (**D**) *In vitro* luciferase activity from *PSMB6* 5′ UTR luciferase reporter mRNA. *PSMB6* is not targeted by eIF3 and undergoes translation shutoff during the ISR. Results are normalized to extracts from untreated cells and represent the mean ± s.d. of three independent experiments.

Figure S5

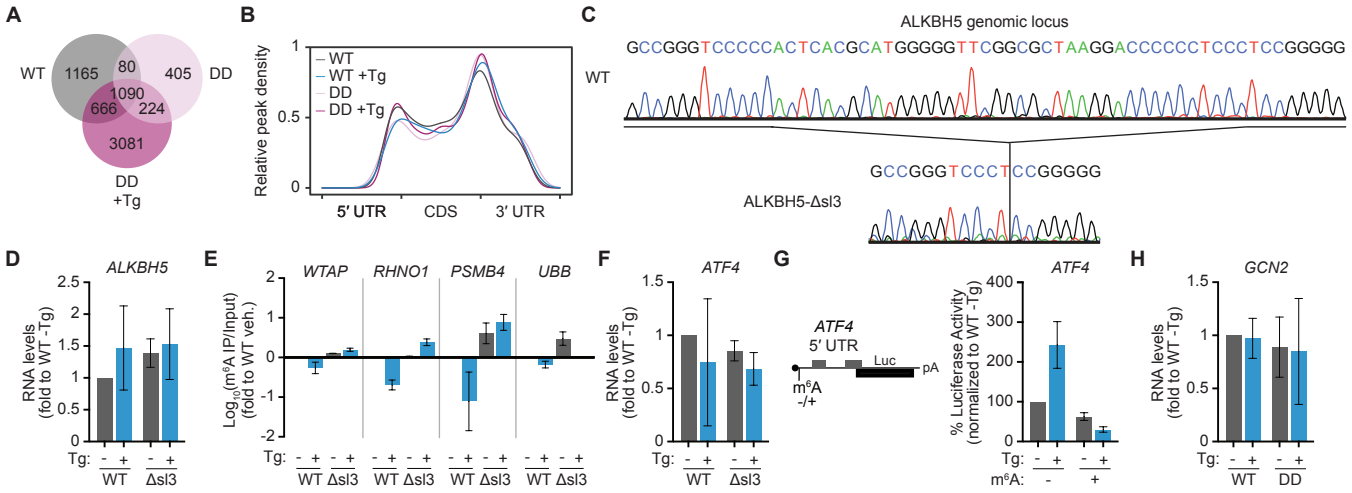
A
WT
1165
80
405
DD
1090
666
224
3081
DD
+Tg
B
Relative peak density
WT
WT +Tg
DD
DD +Tg
5′ UTR
CDS
3′ UTR
C
ALKBH5 genomic locus
GCCGGGTCCCCCACTCACGCATGGGGGTTCGGCGCTAAGGACCCCCCTCCCTCCGGGGG
WT
GCCGGGTCCCTCCGGGGG
ALKBH5-Δsl3
D
ALKBH5
RNA levels (fold to WT -Tg)
Tg:
WT
Δsl3
E
WTAP
RHNO1
PSMB4
UBB
Log10(m6A IP/Input) (fold to WT veh.)
F
ATF4
G
ATF4
5′ UTR
Luc
pA
m6A
-/+
% Luciferase Activity (normalized to WT -Tg)
m6A:
H
GCN2
DD

Figure S5. ISR-regulated mRNA demethylation is dependent on translation regulation of *ALKBH5*, related to Figure 4. (A) Venn diagram of overlapping m^6A-modified transcripts in vehicle or Tg-treated wild-type (WT) and phosphomimetic (DD) eIF3d expressing HEK293T. (**B**) Distribution in transcript regions of all m^6A sites in eIF3d mutant cell lines. UTR, untranslated region; CDS, coding sequence. (**C**) Sanger sequencing validation of genome editing to remove the eIF3 binding site from the ALKBH5 genomic region of HEK293T cells. Shown is chr17 (+): 18,184,106–18,184,164. (**D**) Transcript expression levels of *ALKBH5* are unaffected in cells expressing *ALKBH5* with a mutated 5′ UTR. Δsl3, cells with deletion of the eIF3 binding site in ALKBH5 (Δsl3). (**E**) Levels of m^6A in transcripts in cells with dysregulated eIF3d-specialized translational control of *ALKBH5*. m^6A is measured by m^6A-RIP and qRT-PCR. (**F**) Transcript expression levels of *ATF4* in ALKBH5-Δsl3 cells. (**G**) Luciferase activity *in vitro* mediated by the *ATF4* 5′ UTR is inhibited in the presence of cap-proximal m^6A modification during chronic ER stress. Results are normalized to unmodified RNA in untreated cells. (**H**) Transcript expression levels of *GCN2* are not significantly changed in HEK293T expressing eIF3d mutants. Results in (D–H) are normalized to untreated WT cells and represented as the mean ± s.d. of three independent experiments. Tg treatments were performed for 16 h.

Table S4. Table of oligonucleotides, related to STAR Methods

Oligonucleotide name	Sequence (5′–3′)
CRISPR/Cas9 Editing	
sgRNA ALKBH5	GGCTCTAAGGGGACGCGCCC
sgRNA eIF3d	CTCATCTTCATCAGAGCTGA
Donor ALKBH5	CCACTCACGCATGGGGGTTCGGCGCTAAGGACCCCCCTC CGACCCTAGAGCAGCGTCGTGGGGGCCATGGCGCCGCCA G
Donor eIF3d	CTTCCTCTTCTTCCTCCTCCTCTTCCTCCTCATCTTCATCGT CGTCGAAGGTGCCATCAGGGAGGCTGTAGACACGGATGA CCTGCTTGTTGGGGT
Cloning	
ALKBH5 cloning, SacI-F	GCAGAGCTCTCTGGCTAACTAGAGAACCCACTGCTTACTG GC
ALKBH5 cloning, NheI-R	CCCTCTAGACTCGAGGCTAGCACCGCGGC
ALKBH5 cloning, D-R	GGGGGGCGTCGAGGGTCCGGGC
ALKBH5 cloning, D-F	GACCCTCGACGCCCCCCGCTAAGGACCCCCCTCCCTCCG GG
ALKBH5 cloning, stem-R	GGGGGGCGTCGAGGGTCCGGGC
ALKBH5 cloning, stem-F	CCCTCGACGCCCCCCCGGCCCTCCCCCACTCACGCATGG GGG
ALKBH5 cloning, comp-R	AGGGAGGGGGGTCCTTAGCCGGCTTCCCCCATGCGTG
ALKBH5 cloning, comp-F	CTAAGGACCCCCCTCCCTCCGGGGGG
ALKBH5 cloning, loop-R	GCGCCGAACCCCCAACGCACTCTGGGGGACCCGGC
ALKBH5 cloning, loop-F	TGGGGGTTCGGCGCTAAGGACCC
GCN2 cloning, seq-F	CGAAATTAATACGACTCACTATAAGCGCGGAGCCCCGCCC CGC
GCN2 cloning, seq-R	CATAAACTTTCGAAGTCATGGCAGCGCTGCGCCCAAGGC
ATF4 cloning, seq-F	CGAAATTAATACGACTCACTATACATTTCTACTTTGCCCGC CCAC
ATF4 cloning, seq-R	CATAAACTTTCGAAGTCATGTTGCGGTGCTTTGCTGGAATC G
RT-qPCR	
PSMB6-qPCR-F	CGGGAAGACCTGATGGCGGGA
PSMB6-qPCR-R	TCCCGGAGCCTCCAATGGCAAA
Jun-qPCR-F	TGACTGCAAAGATGGAAACG
Jun-qPCR-R	CAGGGTCATGCTCTGTTTCA
ATF4-qPCR-F	CTTGATGTCCCCCTTCGACC
ATF4-qPCR-R	CTTGTCGCTGGAGAACCCAT
ALKBH5-qPCR-F	CGGCGAAGGCTACACTTACG
ALKBH5-qPCR-R	CCACCAGCTTTTGGATCACCA
FTO-qPCR-F	ACTTGGCTCCCTTATCTGACC
FTO-qPCR-R	TGTGCAGTGTGAGAAAGGCTT
GCN2-qPCR-F	AGGTCTAGGCGAGAACGTCA
GCN2-qPCR-R	CCACTGAAGGACCCACTCAT
TRIB3-qPCR-F	CCGCCCTGGCGCACTGTCAC
TRIB3-qPCR-R	GTCCCACGTAGGCTGGGCAC
ATF3-qPCR-F	GCCACCGGATGTCCTCTGCG

ATF3-qPCR-R	GTTTCGGCACTTTGCAGCTGC
PPP1R15A-qPCR-F	CCGACTGCAAAGGCGGCTCA
PPP1R15A -qPCR-R	CAGCCAGGAAATGGACAGTGAC
ABL1-qPCR-F	GGACTACCGCATGGAGC
ABL1-qPCR-R	CTCACAGCCCCACGGACG
PPP3R1-qPCR-F	CGACACAGATGGGAATGGAGAAGTAGAC
PPP3R1-qPCR-R	GTATCTTTCAGATTGTTCCCCACCATCATCTTCAATAC
FMN2-qPCR-F	GGGCAGTTTCCTAGGCGAGTTCC
FMN2-qPCR-R	CTTCTGGACAGCATCTGAGCGT
WTAP-qPCR-F	GCAACAACAGCAGGAGTCTGC
WTAP-qPCR-R	CTGCTGGACTTGCTTGAGGTAC
RHNO1-qPCR-F	GACCACAGCACCATCACTTCC
RHNO1-qPCR-R	GGTTTTCGACTTGAGTGTCTCG
UBB-qPCR-F	GCCGCACTCTTTCTGACTACAAC
UBB-qPCR-R	CCTCCAGAGTGATGGTCTTGC
PSMB4-qPCR-F	CGCGACTTAGTAGAACGCTGCA
PSMB4-qPCR-R	GTCTCTGTAGACAATGGTCCC
RNA SHAPE analysis	
ALKBH5-SHAPE	GAACCGGACCGAAGCCCGGGGCCTTCGTCTTCGGCCCCC ACGACGCTGCTCTAG